Heterocyclic Letters
Vol. 15| No.1|51-64|Nov-Jan|2025
ISSN : (print) 2231–3087 / (online) 2230-9632
CODEN: HLEEAI
http://heteroletters.org

BENZIMIDAZOLE LEADS THE WAY: STRONGER DNA CONJUGATION, POTENT CANCER AGENT, A STEP AHEAD OF BENZOTHIAZOLE

Uzma Khan[a], Souvik Sur[b*], Dinesh Singh[c], Aaqib Javaid[d], Kshatresh Dutta Dubey[c], Shyam Lal Mudavatdh[d, e]

[a]*Department of Chemistry, Faculty of Engineering, Teerthanker Mahaveer University, Moradabad, Uttar Pradesh-244001, India*
[b]*Research and Development Center, Teerthanker Mahaveer University, Moradabad, Uttar Pradesh-244001, India*
[c]*Department of Chemistry, Shiv Nadar University, Greater Noida, Uttar Pradesh-201314, India*
[d]*Institute of Nano Science and Technology, Knowledge City, Sector 81, Mohali, Punjab*
[e]*Department of Animal Sciences, University of Hyderabad, India*
**Corresponding author's E-mail: drsouvik.engineering@tmu.ac.in*

Abstract
Benzimidazole shows certain advantages over Benzothiazole, whether in terms of stronger DNA binding, higher anti-cancer efficacy, or broader therapeutic applications. This study assesses the stability of BNZ-AC, based on Benzimidazole moiety conjugated to polyA$_{15}$polyT$_{15}$-DNA system in comparison to three other DNA-conjugated systems. Among all four systems, the conjugated DNA with BNZ-AC demonstrated the most favourable interaction, as indicated by a notable thermal stability increase of 6.54 ˚C and the Gibbs free energy of -19.75 kcal/mol, making it the most stable ligand, surpassing BTZ-AC, and DM-BTZ-AC, based on Benzothiazole in terms of binding affinity. Molecular dynamics simulations further supported BNZ-AC's enhanced stability through consistent hydrogen bonding patterns. Moreover, cytotoxicity assays revealed that BNZ-AC exhibited potent activity against Hela cells with a low IC$_{50}$ of 8.012 µM, although it was less effective against A549 cells, showing an IC$_{50}$ of 69.5 µM. These results indicate that BNZ-AC holds promise as a therapeutic candidate due to its strong DNA binding, superior stability, and significant cytotoxic activity against cancer cells, thus Benzimidazoles edges over Benzothiazole analogues.

Keywords: Benzimidazole, Benzothiazole, DNA-conjugate, DNA thermal stability, Molecular Dynamics, Cell viability assay.

1. Introduction

Interaction with bioactive small organic molecules like Benzimidazole and Benzothiazole has attracted much interest. Many studies on DNA conjugation have been performed because of its applications in drugs, diagnostics, and cancer treatment. The compounds discussed in this article, Benzimidazole and Benzothiazole are heterocyclic compounds meaning that, they

contain nitrogen and combination of nitrogen-sulfur atoms respectively as hetero atoms. They can accommodate themselves against DNA by using method such as intercalation and groove binding due to the fact that they have planar structures. These interactions are critical for the discovery of therapeutic agents that can modulate the DNA processes including replication and transcription. Research has revealed that these compounds can prevent cancerous cell growth by interacting with DNA and interposing with significant cell processes. For example, Benzimidazole derivatives show potent anti-tumour activities that involve inhibiting the polymerisation of Tubulin. Benzothiazole compounds cause selective DNA topoisomerases inhibition which essential for facilitating DNA-unwinding and replication (i). Furthermore, these molecules have been examined for application in diagnostics where potential of these compounds can be used in conjugation with DNA probes to facilitate the identification of particular gene sequences (ii). The future prospects of Benzimidazole and Benzothiazole conjugated compounds include the generation of new and improved treatments based on molecular targeting and the rational design of drugs for personalized medicine. DNA conjugation to small molecules and tissues such as Benzimidazole and Benothiazole has limitations such as off-target effects due to the rigidity of the DNA structure and poor cellular uptake. Furthermore, accurate targeting and site-controlled release of pharmaceutical substances have not yet been solved fully in therapeutic systems (iii).

In the arena of chemotherapeutics, the identification of specific DNA sequences by small molecules is gradually assuming the position of paramount significance (iv-vi). Substances such as pyrroles, imidazoles, polyamides, polybenzamides, furans, diamidines, carbazoles, and pyrroloindoles are well-known DNA sequence-selective binders to human genomic DNA (vii-viii).These molecules often have a crescent shape, which allows them to fit precisely into the major or minor grooves of DNA, enabling isohelical alignment. This precise binding facilitates the selective targeting of DNA sequences, offering a powerful strategy for controlling gene expression in cells. Structural studies of these small molecules are crucial, as they can provide insights into their DNA binding mechanisms, opening new avenues for developing therapeutic tools that regulate gene expression by manipulating DNA sequence recognition. This approach holds significant potential for advancing personalized medicine and developing more effective cancer treatments (ix).

Hurley reported that many anticancer drugs target DNA, with anti-tumor antibiotics often displaying specific DNA interactions (x). Given the lack of prior studies on DNA recognition by certain compounds, there is keen interest in exploring these interactions. Hoechst and other minor groove ligands, like benzimidazole-based molecules, are known to bind specifically to AT/GC sequences (xi-xiv). The sequence-specific binding of bisbenzimidazoles to AT-rich DNA has been previously examined by our groups, highlighting the importance of systematic studies in understanding drug-DNA interactions (xv-xviii). DNA-small compound conjugates have emerged as versatile tools in biomedicine, owing to the unique properties of both DNA and small molecules. The conjugation of DNA with small compounds provides a multifunctional platform that can be tailored for various applications, including targeted drug delivery, molecular diagnostics, imaging, and bio sensing.

One of the primary advantages of DNA-small compound conjugates is the combination of DNA's inherent ability to recognize specific sequences through base pairing with the functional properties of small molecules. This allows for the precise targeting of biological processes. For example, DNA-drug conjugates have been explored for targeted drug delivery. Studies have demonstrated that by attaching chemotherapeutic agents, such as doxorubicin, to DNA, it is possible to achieve selective delivery to cancer cells with minimal off-target effects. The DNA acts as a carrier, while the drug remains inactive until it reaches the target

site, where it can be released either through enzymatic cleavage or environmental triggers like changes in pH (xix).

The other major application of DNA-small compound conjugates is in diagnostics and imaging where they also appear to have potential. Based on the fact that DNA can bind to various small fluorescent dyes, it has facilitated the identification of particular nucleic acid sequences in a cell or tissue. For instance, DNA-dye conjugates have been applied into the fluorescence in situ hybridization (FISH) approach for the detection of existence of abnormalities of the genome with high throughout (xx). In addition; these conjugates have been used in the synthesis of biosensors for analyzing biomolecules including proteins and nucleic acids from body fluids. To enhance the selectivity of the developed sensors, researchers have confined a target analyse to interact with a small molecule attached to a DNA strand (xxi). More than that, in recent years, the auxiliary of DNA-small compound conjugates in nanotechnology has broadened the range of application. Many small attachment compound molecules covalently bonded to the DNA-functionalized nanoparticles are under the evaluation for better drug delivery since the nanoparticles can be designed to release the therapeutic agent to the target site only at the specific stimulus such as light or magnet (xxii).

Nevertheless, some problems are still relevant to the current state of knowledge, for example, the improvement of the stability and compatibility of these conjugates in biological media. However, the current research is still in progress to enhance these systems; thus, it can be predicted that DNA-small compound conjugates will be shown to have huge future potential in the development of precision medicine, diagnostics. DNA-small compound conjugates constitute an exciting growing area of research and application in the context of expanding medical and biotechnological applications of DNA that integrates the marvelous selectivity of DNA with the chemical versatility of small molecules.

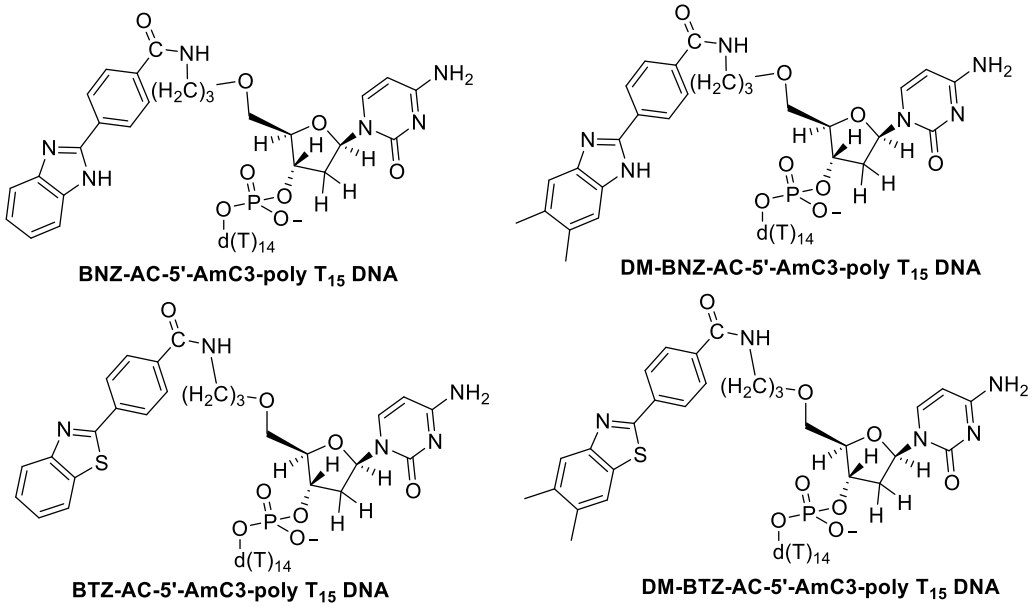

Figure 1: Structure of DNA Conjugates

In this study, the DNA sequence (AT-rich) recognition capabilities of four heterocyclic molecules, BNZ-AC, DM-BNZ-AC, BTZ-AC and DM-BTZ-AC, based on benzimidazole/benzothiazole moieties (**Figure 1**), are investigated using techniques like thermal denaturation, molecular docking, and cell viability assays against cancer cell lines. Since these compounds are derived from benzimidazole and benzothiazole, their ability to recognize specific DNA sequences could lead to significant insights, potentially informing the development of more effective drugs with improved sequence selectivity.

1. 2. Experimental Procedure

2.1 Synthesis of DNA-conjugates

The compounds BNZ-AC, DM-BNZ-AC, BTZ-AC, and DM-BTZ-AC were synthesized by reported procedure (xxiii-xxvi). All the synthesized compounds were further purified by column chromatography and characterized through NMR, IR, mass spectrometry etc. All four compounds were further coupled with poly-T DNA with 5'-modification as C3-linker (5'AmC3-poly T DNA) which was earlier reported by our previously published article (xxv). The purified compounds were directly use for all experiments. The complementary poly-A_{15} DNA sequence was procured from Sigma Aldrich in HPLC grade and the working buffer 10 mM sodium cacodylate buffer at pH=7.0 was made with standard protocol.

2.2 Thermal melting determination of DNA

The construction of thermodynamic models and the analysis of potential structural biopolymer conformations depend heavily on the thermal measurements of DNA. The present study examined the structural stability of DNA in the presence of ligands using thermal denaturation. The number of helical areas and the number of untwisted regions are identical when the temperature approaches the melting point (T_m). T_m, then, is the temperature where 50% of a DNA sequence is in the helix shape and the remaining 50% is not. A further rise in temperature causes a significant shift in equilibrium in favor of a rise in the proportion of single strands. Increased UV absorption intensity occurs along with this process. The relationship between UV absorption intensity and temperature is shown by the melting curve. Using a UV spectrophotometer, melting curves of poly-nucleotides with fixed (Compound/DNA=1:1) concentrations were observed at a fixed wavelength of 260 nm, which is the wavelength at which DNA absorbs the most energy. We have used 10 mM sodium cacodylate buffer at pH=7.0 in the whole experiments. The poly-A_{15} DNA were initially hybridized with complementary other four Conjugated-poly-T_{15} DNA by heating on a water bath from 10-95 °C and then cooled to room temperature and finally keeping those duplex DNAs overnight in freezer.

2. 2.3 Computational Details

This computational study employed a multi-step approach to investigate the interaction between ligand molecules and their target binding sites. Harnessing the power of density functional theory (DFT) for drug design, we initiated our study with a comprehensive optimisation of ligand molecules using Gaussian-09. This approach ensures an accurate balance between computational efficiency and the quality of electronic structure calculations, particularly for medium-sized organic molecules like drugs. The B3LYP/6-31G level of theory is well-suited for predicting the molecular geometry, electronic properties, and stability of the drug candidates, providing a reliable foundation for subsequent docking and molecular dynamics simulations. This method facilitates the identification of the most favourable binding pose, which is then further explored using molecular dynamics (MD) simulations for 50ns. For this purpose, the AMBER-22 package (xxvii) was employed, allowing for a detailed investigation of the drug-protein interactions at an atomistic level. This MD approach is not only effective in predicting binding affinities but also provides deep insights, contributing to the rational design of more effective drug candidates.

Following the molecular dynamics simulations, we performed a Molecular Mechanics Poisson-Boltzmann Surface Area (MMPBSA) analysis (xxviii-xxix) to evaluate the stability of the drug molecules within the binding site. MMPBSA is a widely used post-simulation technique that provides insights into the binding free energy of ligand-protein complexes by considering both molecular mechanics and solvation energy contributions. We also calculated the Gibbs free energy for each system, which provides a quantitative measure of the thermodynamic stability of the drug within the active site. By analysing the Gibbs free

energy, we could determine how favourable the binding is under physiological conditions. A more negative Gibbs free energy corresponds to a stronger, more stable interaction between the drug and the target protein, thereby validating the docking and MD simulation results.

3. System Preparation

The initial coordinates for the DNA structure were sourced from the duplex structure of B-DNA from SCFBIO Web server (http://www.scfbio-iitd.res.in/software/drugdesign/bdna.jsp). Using the tleap module of the AMBER22 package and the ff19SB force field (xxx), we meticulously prepared the system by adding missing hydrogen atoms and neutralizing the structure through the addition of counter ions. This crucial step ensures the stability and accuracy of the molecular dynamics simulations, enabling realistic modelling of the DNA-ligand interactions. All four ligands BNZ-AC, DM-BNZ-AC, BTZ-AC and DM-BTZ-AC were utilized to position at the 5'-end of polyA_{15}polyT_{14} at the place of terminal thymine (T). The force field parameters for all four ligands were generated using the General Amber Force Field 2 (GAFF2) (xxxi) in the Antechamber module, ensuring compatibility with the AMBER force field for subsequent MD simulations. The geometry of each ligand was optimized at the B3LYP/6-31G level of theory to achieve accurate molecular conformations, which are critical for the simulation's reliability and the interaction study.

4. MD Simulation

The MD simulations were initiated following system preparation, where the ligand-DNA complexes were solvated in an explicit water box with counter ions added to neutralize the system. After preparation, energy minimization was performed to remove any unfavourable contacts, ensuring a stable starting structure. The system was gradually heated to 300 K using the Langevin thermostat with weak restraints applied to the solute. After reaching the target temperature, equilibration was conducted in the NPT ensemble, maintaining constant pressure and temperature using a Berendsen barostat. During the production phase of the MD simulations, a time step of 2 fs was used to integrate the equations of motion, with coordinates saved at regular intervals to analyse the system's behaviour over time. The Particle Mesh Ewald (PME) method (xxxii) was employed to accurately treat long-range electrostatic interactions, while the SHAKE algorithm constrained all bonds involving hydrogen atoms, allowing for a larger time step without compromising accuracy.

Analysis of the MD trajectories involved calculating the Root Mean Square Deviation (RMSD) to monitor the overall structural stability of the complex, and Root Mean Square Fluctuation (RMSF) to assess the flexibility of specific residues or regions of the system. Radial distribution functions and hydrogen bond analysis were also performed to explore key interactions between the drug molecules and the receptor over the simulation period. Furthermore, MMPBSA calculations were performed on snapshots extracted from the trajectory to evaluate the binding free energy of the complexes, providing insights into the stability and energetics of the drug-target interactions during the simulation.

3.4 Cell Viability Assay

The cytocompatibility of substances was evaluated on the Hela and A549 cell lines using the 3-[4,5-dimethylthiazol-2-yl]-2,5-diphenyl tetrazolium bromide (MTT) test (xxxiii-xxxiv). Cells (5×10^4 cells/well) were injected into 96-well plates and adhered for 24 hours at 37 ± 2 ºC in a 5% CO_2 environment. Cells were exposed to formulations (BNZ-AC, DM-BNZ-AC, BTZ-AC, DM-BTZ-AC) at several doses (ranging from 400 µg/mL to 12.5 µg/mL), with untreated cells serving as a control group. After that, we injected 20 µL of MTT reagent (5 mg/mL) each well and incubate for 4 hours. Each well was treated with DMSO to dissolve the formazan crystals. The optical density (OD) was measured at 570 nm with a microplate reader (Infinite 200 PRO). All experiments were done in triplicates.

3. Results and Discussions:

3.1 Synthesis of Benzimidazole and Benzothiazole DNA-Conjugates:

Two derivatives of Benzimidazoles named BNZ-AC and DM-BNZ-AC, were synthesized using known methods reported in literatures (xxiii-xxiv). On the other hand, two analogues BTZ-AC and DM-BTZ-AC were also prepared using same protocols. Synthesized compounds were characterized through NMR, IR and Mass spectrometry. The synthesis protocols of all four conjugates polyT_{15}-BNZ-AC-DNA, polyT_{15}-DM-BNZ-AC-DNA, polyT_{15}-BTZ-AC-DNA and polyT_{15}-DM-BTZ-AC-DNA was earlier reported (xxv-xxvi).

3.2. Thermal melting Experiment of DNA-conjugate systems

The data presented in the table (**Table 1**) highlights the effect of different ligands on the melting temperature (T_m) of a DNA duplex with and without conjugations, a crucial factor in understanding the stability of DNA's double-stranded structure.

Table 1: DNA-melting Temperatures:

System	T_m (°C)	$\triangle T_m$(°C)
polyA_{15}polyT_{15}-DNA	38.05	-
polyA_{15}polyT_{15}-BNZ-AC-DNA	44.59	6.54
polyA_{15}polyT_{15}-DM-BNZ-AC-DNA	43.56	5.51
polyA_{15}polyT_{15}-BTZ-AC-DNA	41.38	3.33
polyA_{15}polyT_{15}-DM-BTZ-AC-DNA	42.37	4.32

T_m is, therefore, the temperature at which 50% of the DNA base pairs are melted, and thus it is very essential in identifying the effects of outside molecules such as ligands on DNA stability. After conjugation with DNA they can either restabilize or destablize its structure which results in change in the T_m. The table shows that various ligands have different impacts on the T_m of the DNA duplex, according to the variables of their interactions. For instance, the ligand BNZ-AC stabilized the T_m and the ‘‘melting temperature’’ showed an increase of 6.54 °C. Such a great increase means that BNZ-AC is able to increase the stability of DNA duplex, likely through the formation of stable covalent bonds or molecular rigidity imparting structures that are less likely to be denatured. This appears to indicate a very positive cooperative conformation with the DNA in the presence of the BNZ-AC, resulting in the raising of its overall thermal stability (**Figure 2**). On the other hand, the effect of BTZ-AC on T_m was more fluctuating and was found to have a slightly elevated T_m of just 3.33 °C. This smaller increment infers a poor or complicated participation of BTZ-AC with the DNA duplex. These fluctuations in the T_m effect suggest that perhaps, BTZ-AC is not stabilizing the DNA equally or that the interaction is variable and may depend on the structural characteristics of the DNA sequence.

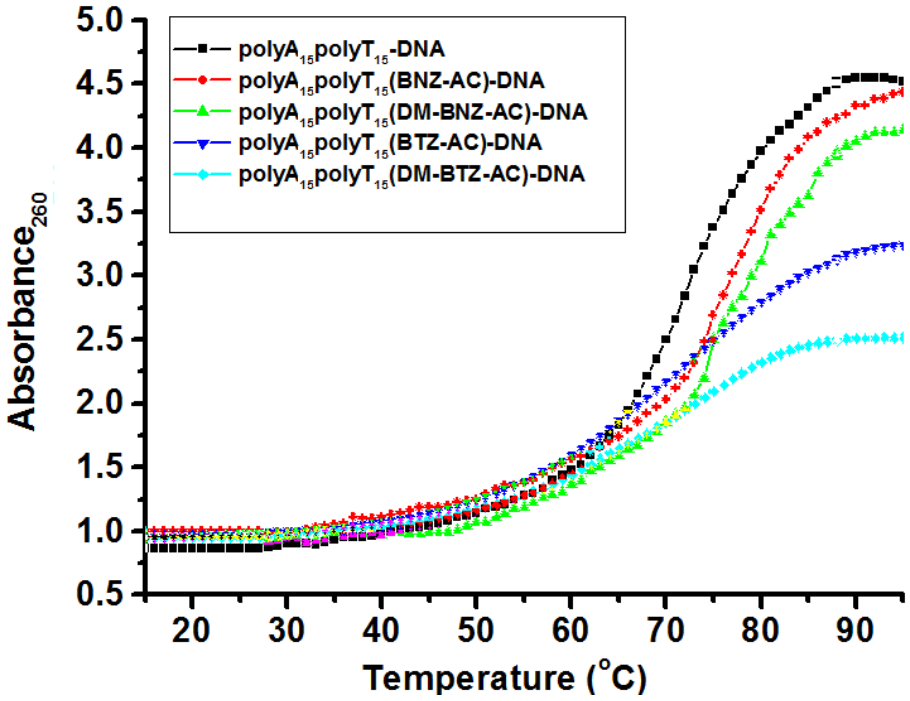

Figure 2: Thermal denaturation plots of DNA systems with and without ligands with details of melting temperatures

Moreover, the ligands DM-BNZ-AC and DM-BTZ-AC showed moderate impact towards T_m enhancing the T_m about 5.51 °C and 4.32 °C respectively. These values indicate that both ligands fix the polyA$_{15}$polyT$_{15}$-DNA system to some extent after the conjugation, but not as effectively as BNZ-AC. The moderate increase in T_m for these ligands means that, even though they promote individual DNA stability, their ability to interact with DNA is not as strong as might be expected, revealing that there are some differences in their structure or affinity.

5. 3.3. MD Simulation of DNA-ligand complexes

Besides the docking studies, the overall stability of the ligand-DNA complexes was further assessed by RMSD and RMSF. These analyses give information about the behaviour of the docked ligands in the course of the simulation. The RMSD values quantify the general displacement in the ligands from their original conformation, and the RMSF values are greatly helpful to understand the fluctuation of residues throughout the system. As seen from the RMSD and RMSF analyses, there were marginal changes in every of the four conjugated DNA systems containing BNZ-AC, DM-BNZ-AC, BTZ-AC and DM-BTZ-AC revealing that the ligands remained well anchored in their binding sites.

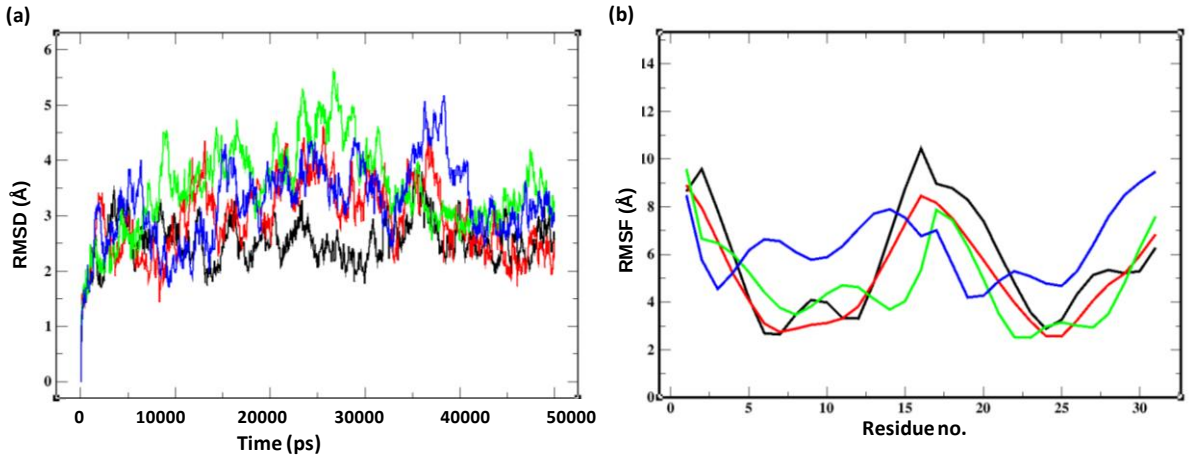

Figure 3: (a) RMSD and (b) RMSF plot for BNZ-AC (in black), DM-BNZ-AC (in blue), BTZ-AC (in green) and DM-BTZ-AC (in red)

The low variance found in the RMSD and RMSF values for all systems is quite striking as it argues for steady interactions of the ligands with the DNA throughout the simulation process. These outcomes also corroborate the generic docking scores to imply that indeed, the binding affinities inferred from the docking analysis are feasible complexes. As Figure 3, the RMSD graph show the help of each system in detail while highlighting structural stability of the ligands at the end of simulation. These docking and simulation analyses collectively point towards the stability of the ligand-DNA interactions, and therefore can be further explored.
After the system preparation, the conjugated thymine moiety at the 5' position of DNA strand was gently transformed to the non-conjugated counterparts. As part of the investigation on the stability of the modified DNA structure, RMSD and RMSF were calculated. The analyses of these results showed that the DNA had negligibly small variations and deviations about a value that characterized the structural stability of the molecule during the simulation. The negligible variation in the RMSD and RMSF values further justified the stability of the system that was used to analyzed the DNA structure; this meant that non-conjugated thymine at the 5' end did not pose any threat to the stability of the designed model.

4.1 MM-PBSA Calculations

To analyze DNA structure and support our assessment of binding energies, we conducted MMPBSA calculations. This approach enables identification of the Gibbs free energy (ΔG) of binding, which is essential in comprehending the strength and stability of ligand-DNA interactions. The Gibbs free energy values which were calculated for the ligands BNZ-AC, DM-BNZ-AC, BTZ-AC and DM-BTZ-AC were -19.75 Kcal/mol, -14.37 Kcal/mol, -7.04 Kcal/mol, -16.01 Kcal/mol respectively. These negative values show that the binding of the ligands to the DNA is thermodynamically favorable for this system and that the more negative value the better the binding interacted.

Table 2: MM/PBSA binding energy computation of the DNA-systems receptor complex

System	ΔE_{vdw}	ΔE_{ele}	ΔG_{Gas}	ΔG_{Solv}	ΔG_{Free}
$polyA_{15}polyT_{15}$-BNZ-AC-DNA	-12.19±2.16	-19.13±1.18	-60.91±5.75	41.16±4.24	-19.75±2.59
$polyA_{15}polyT_{15}$-DM-BNZ-AC-DNA	-1.09±0.36	-28.74±4.59	-48.01±4.71	33.63±4.22	-14.37±1.50
$polyA_{15}polyT_{15}$-BTZ-AC-DNA	-0.36±0.64	-39.77±3.55	-51.45±3.04	44.40±3.10	-7.04±1.54
$polyA_{15}polyT_{15}$-	-	-	-	48.79±6.25	-

DM-BTZ-AC-DNA	11.06±1.88	40.79±6.10	64.79±6.86	16.01±0.42

*All energies are calculated in kcal mol^{-1}

MMPBSA calculations are of great use in computational chemistry since they provide the decomposition of binding free energy into different terms. The method incorporates molecular mechanics (MM) with solvation models like Poisson-Boltzmann (PB) or Generalized Born (GB), with surface area analysis for the appraisal of non-bonded forces between molecules. Some other non-bonded interactions are vdW forces and electrostatic contributions that would allow assessing how well a ligand fits into the binding pocket and, correspondingly, how well it interacts with the surrounding environment. The solvation energy, another factor, defines how solvent influences the binding, making MMPBSA a valuable approach for biological systems, including the ligand-DNA complex. In the context of our study, with MMPBSA calculations it was possible to break down the energy into more concrete terms. While the van der Waals energy is the energy result of close contact between a ligand and atoms of the DNA molecule, the electrostatic energy is an indication of the Coulombic interactions between charged or polar zones of the ligand and the DNA molecule. Additionally, solvation energy is split into polar and non-polar contributions: the polar contribution arises from the solute solvent electrostatic interactions obtained from Poisson Boltzmann equation and the nonpolar contribution arises from the solute solvent surface area interaction.

From the results above, we analyzed the Gibbs free energy of each of the presented hybrid DNA complexes with BNZ-AC, DM-BNZ-AC, BTZ-AC and DM-BTZ-AC and studied the hydrogen bonding interactions within the DNA-conjugated complexes for the better understanding of the binding condition. Specific to the hydrogen bonds, they are highly important in stabilizing the given ligand receptor interactions and the amount of hydrogen bonds present can strongly affect the given type of binding affinity. In the course of the entire MD simulation, we remained constant with hydrogen bonding pattern for BNZ-AC ligands more in compare to the other three remaining ligands indicating that such interaction is rather critical for the stability of the complex. We observed the formation and stability of hydrogen bond between the ligands and essential amino acids of the DNA binding pocket of each ligand. The analysis of the data provided by the software was indicative of the formation of hydrogen bonds throughout the simulation except for the ligands. This is in concordance with the negative Gibbs free energy values determined earlier, because the hydrogen bonding interaction supports the favourability of the binding process. The stability of these bonds also reveals that the ligands can remain stable within the binding site throughout an application, which is beneficial in biological systems.

The results from the Gibbs free energy calculations reinforce the conclusions drawn from docking and stability analyses. The more negative the Gibbs free energy, the more favourable the binding interaction. For instance, the ligands BNZ-AC, DM-BNZ-AC and BTZ-AC exhibit relatively strong binding with ΔG values around -19.75 kcal/mol, while BTZ-AC shows a comparatively weaker binding interaction with a value of -7.04 kcal/mol (**Table 2**). This difference in binding strength could be attributed to variations in how each ligand interacts with the DNA at the atomic level, such as differences in van der Waals forces or electrostatic interactions. Overall, these MMPBSA results provide a nuanced understanding of ligand stability and binding strength, giving us a deeper insight into the molecular interactions that govern the behaviour of these complexes.

4.2 Hydrogen bonding patterns

After determining the Gibbs free energy for each hybrid DNA complexes with BNZ-AC, DM-BNZ-AC, BTZ-AC and DM-BTZ-AC, we further investigated the hydrogen bonding interactions within the DNA-conjugated complexes to deepen our understanding of the binding mechanisms. Hydrogen bonds are essential in stabilizing ligand-receptor interactions, and their presence can significantly contribute to the overall binding affinity. Throughout the entire molecular dynamics simulation, we observed consistent hydrogen bonding patterns for BNZ-AC ligands more in compare to the other three remaining ligands, suggesting that these interactions play a crucial role in maintaining the stability of the complex. We monitored the formation and persistence of hydrogen bonds between the ligands and key residues within the DNA binding site for each ligand. The results showed that hydrogen bonds were formed consistently during the simulation, further confirming the ligands' stable binding (Figure 4). This observation aligns with the negative Gibbs free energy values previously calculated, as the hydrogen bonding interactions contribute to the overall favourability of the binding process. The persistence of these bonds also indicates that the ligands can effectively maintain their position within the binding site over time, potentially improving their efficacy in biological settings.

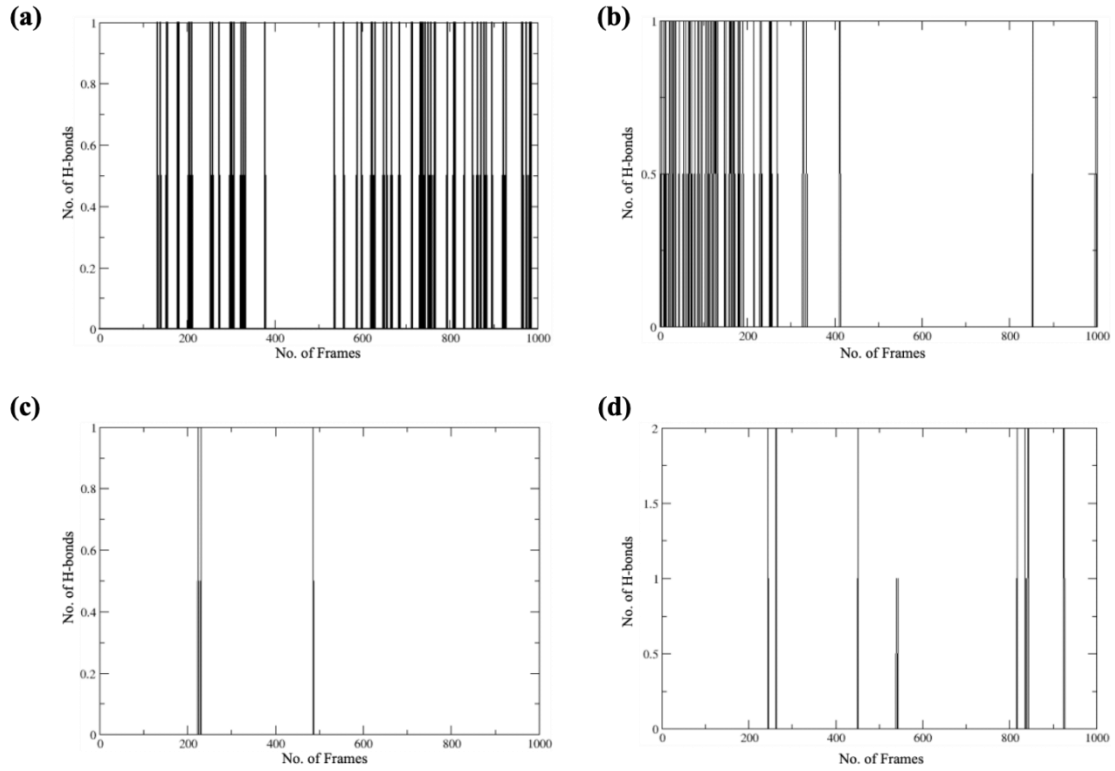

Figure 4: Hydrogen bonding pattern found during the MD Simulation for (a) BNZ-AC, (b) DM-BNZ-AC, (c) BTZ-AC, and (d) DM-BTZ-AC

This presence of strong hydrogen bonding also extends across the various ligand systems, which implies more than just structural reinforcement of the DNA; but also increases the interaction between the ligands and DNA. From the protein-protein docking, the hydrogen bonding that result from the docking exercise creates specific and directional interactions that support the docking scores and the MMPBSA outcomes. These results are quite enlightening as they draw attention to hydrogen bonding interactions as the molecular recognition processes which could be adopted in developing enhanced selectivity and potency of

therapeutic ligands. This is different from focusing on only energetic elements of ligands with their targets, as well as the use of factors such as hydrogen bond interactions.

3.4. Cytocompatibility assay

The Table 3 presents the IC_{50} data (half maximal inhibitory concentration) for four compounds tested against two cell lines: Hela, cervical cancer cells and A549, lung cancer cells. The IC_{50} data of four compounds (BNZ-AC, DM-BNZ-AC, BTZ-AC, and DM-BTZ-AC) were analyzed against two cell lines: Two cell lines; Hela – cervical cancer cell line and A549 – lung cancer cell line. BNZ-AC has the best result with a very low IC_{50}, that is 8.012 µM against Hela cells.

Table 3: IC_{50} of the compounds

Compound Entry	Hela	A549
BNZ-AC	8.012	69.5
DM-BNZ-AC	49.58	180.4
BTZ-AC	22.92	160.2
DM-BTZ-AC	33.05	161.6

Again it is less potent against A549 cells where the IC_{50} value is found to be 69.5 µM. DM-BNZ-AC has the lowest potency for both cell lines as it require relatively high concentration to exert the same response as the most potent compound with IC_{50} of 49.58 µM for Hela and 180.4 µM for A549. The compound displays moderate activity with the respective CSF antigene values of BTZ-AC amounting to IC_{50} of 22.92 µM in Hela and 160.2 µM in A549. DM-BTZ-AC also revealed moderate activity with the IC_{50} of 33.05 µM for Hela and 161.6 µM for A549 indicating that this compound has slightly higher activity than BTZ-AC for Hela and has comparable activity for A549.

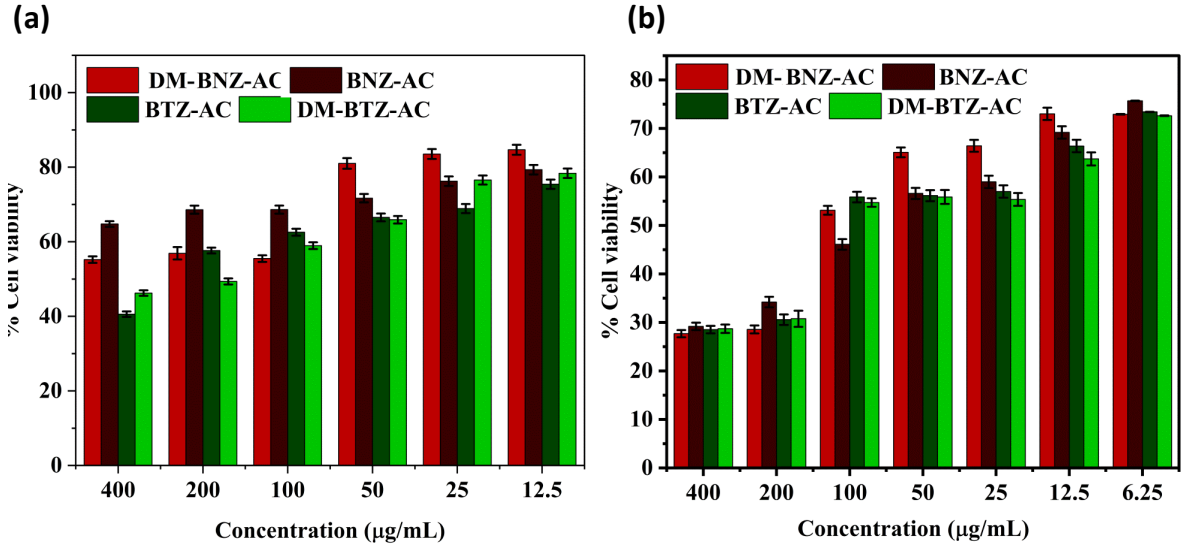

Figure 5 Cyto-compatibility of various formulations (a) in Hela cell lines and (b) A549 Cell lines in different concentrations

In conclusion, BNZ-AC is the most active compound especially on Hela cells. The other compounds are considerably less effective, requiring much higher concentrations of the inhibitors and exhibiting especially a high IC_{50} value for A549 cells. Based on this data BNZ-AC can be considered as the strongest candidate for additional studies of further cancer treatment. The figure shows cytocompatibility of four formulations (DM-BNZ-AC, BNZ-AC, BTZ-AC and DM-BTZ-AC) on Hela human cervical cancer cell line and A549 human lung cancer cell lines at different concentrations ranging from 400µg/mL to 12.5µg/mL. The weakest cell viability was observed when using the BNZ-AC in high concentrations;

moreover, the maximum cytotoxicity of the compounds was as follows: BNZ-AC > BTZ-AC > DM-BTZ-AC. Among the three concentrations, DM-BNZ-AC is least effective as we find higher cell viability at these concentrations. With the dilution, cell viability raises for all compounds, which indicate no significant dissimilarities in cell viability at the lowest concentration (12.5 µg/mL). Similar observation is found in A549 cell line where BNZ-AC provides the best yield of the inhibitory effect decreasing the cell viability at a concentration of 400 µg/ ml and 200 µg/ ml. Here, DM-BNZ-AC has increased cell viability over all concentrations thus suggesting less cytotoxicity as compared to the other synthesized products. Dose–response plots for all compounds in both cell lines showed that at 12.5 µg/mL cell viability is higher and it points to dose dependent cytotoxicity. Combined, BNZ-AC exhibits the highest ability to suppress the viability of cells relative to control and DM-BNZ-AC, with the lowest ability to kill more cells and the highest ability to keep cells alive. The results presented reveal the differences in cytotoxicity of the formulations, with BNZ-AC yielding the highest toxicity, particularly in high concentrations.

4. Conclusion

BNZ-AC demonstrates a strong and favourable interaction when conjugated with polyA_{15}polyT_{15}-DNA system among the four DNA-conjugate systems, indicated by a significant rise in thermal stability of 6.54 ˚C and a Gibbs free energy value of -19.75 kcal/mol, which is the lowest among the studied ligands. This suggests superior stability and binding affinity compared to DM-BNZ-AC (-14.37 kcal/mol), BTZ-AC (-7.04 kcal/mol), and DM-BTZ-AC (-16.01 kcal/mol). Consistent hydrogen bonding patterns observed during molecular dynamics simulations further reinforce BNZ-AC's enhanced stability. Additionally, BNZ-AC exhibits the most potent cytotoxic activity against Hela cells, with a low IC_{50} of 8.012 µM, though it is less effective against A549 cells, with an IC_{50} of 69.5 µM. These findings highlight BNZ-AC's potential as a promising therapeutic candidate. In summary, benzimidazole proves to be a promising candidate in cancer treatment, showcasing stronger DNA binding, potent anti-cancer effects, and a distinct edge over benzothiazole.

5. Acknowledgement:

UK is thankful to Teerthanker Mahaveer University, Moradabad for financial assistance and facility available for her research work. SS is also thankful to the facility provided by Teerthanker Mahaveer University, Moradabad, Uttar Pradesh, India and granting seed money for the completion of this project via ref. TMU/R.O./2020-21/Seed money/002 dated 19/06/2021.

6. Competing Interest

The Authors declare no conflict of interest.

7. Reference

i. Venugopal, S., Kaur, B., Verma, A., Wadhwa, P., Magan, M., Hudda, S., & Kakoty, V. Recent advances of benzimidazole as anticancer agents. *Chemical Biology & Drug Design*, 2023, **102(2)**, 357-376.

ii. Sharma, P. C., Sharma, D., Sharma, A., Bansal, K. K., Rajak, H., Sharma, S., & Thakur, V. K. New horizons in benzothiazole scaffold for cancer therapy: Advances in bioactivity, functionality, and chemistry. *Applied Materials Today*, 2020, **20**, 100783.

iii. Kulkarni, J. A., Witzigmann, D., Thomson, S. B., Chen, S., Leavitt, B. R., Cullis, P. R., & van der Meel, R. The current landscape of nucleic acid therapeutics. *Nature nanotechnology*, 2021, **16(6)**, 630-643.

iv. Patil, S. D., Rhodes, D. G., & Burgess, D. J. DNA-based therapeutics and DNA delivery systems: a comprehensive review. *The AAPS journal*, 2005, **7**, E61-E77.

v. Khanna, A. DNA damage in cancer therapeutics: a boon or a curse? *Cancer*

research, 2015, ***75*(11)**, 2133-2138.

vi. Anchordoquy, T. J., Allison, S. D., dC Molina, M., Girouard, L. G., & Carson, T. K. Physical stabilization of DNA-based therapeutics. *Drug discovery today*, 2001, **6(9)**, 463-470.

vii. Houck, C. M., Rinehart, F. P., & Schmid, C. W. A ubiquitous family of repeated DNA sequences in the human genome. *Journal of molecular biology*, 1979, **132(3)**, 289-306.

viii. Dunham, I., Hunt, A. R., Collins, J. E., Bruskiewich, R., Beare, D. M., Clamp, M., & Ren, Q. The DNA sequence of human chromosome 22. *Nature*, 1999, **402(6761)**, 489-495.

ix. Warren, C. L., Kratochvil, N. C., Hauschild, K. E., Foister, S., Brezinski, M. L., Dervan, P. B., & Ansari, A. Z. Defining the sequence-recognition profile of DNA-binding molecules. *Proceedings of the National Academy of Sciences*, 2006, **103(4)**, 867-872.

x. Hurley, L. H. DNA and its associated processes as targets for cancer therapy. *Nature Reviews Cancer*, 2002, **2(3)**, 188-200.

xi. Pjura, P. E., Grzeskowiak, K., & Dickerson, R. E. Binding of Hoechst 33258 to the minor groove of B-DNA. *Journal of Molecular Biology*, 1987, **197(2)**, 257-271.

xii. Harshman, K. D., & Dervan, P. B. Molecular recognition of B-DNA by Hoechst 33258. *Nucleic acids research*, 1985, **13**, 4825-4835.

xiii. Singh, M. P., Joseph, T., Kumar, S., Bathini, Y., & Lown, J. W. Synthesis and sequence-specific DNA binding of a topoisomerase inhibitory analog of Hoechst 33258 designed for altered base and sequence recognition. *Chemical research in toxicology*, 1992, **5(5)**, 597-607.

xiv. Peñalver, P., Abdelouahid, S., Bosch, P., Hunter, C. A., & Vicent, C. A Neutral DNA Sequence-Selective Vector for Interaction Studies: Fluorescence Binding Experiments Directed Towards a Carbohydrate-DNA Carrier. 2008.

xv. Singh, M., Sur, S., Rastogi, G. K., Jayaram, B., & Tandon, V. Bi and tri-substituted phenyl rings containing bisbenzimidazoles bind differentially with DNA duplexes: a biophysical and molecular simulation study. *Molecular BioSystems*, 2013, **9(10)**, 2541-2553.

xvi. Sur, S., & Khan, U. The Compatibility of Benzimidazole and Benzothiazole derivatives towards poly-A. poly-T DNA. *Indian Journal of Chemistry (IJC)*, 2024, **63(1)**, 65-71.

xvii. Khan, U., & Sur, S. Exploring DNA Binding of Benzothiazole-based Known Drugs: A Molecular Docking Investigation, 2023.

xviii. Khan, U., & Sur, S. (2024, October). Exploring the DNA Recognition of Compounds Based on Benzimidazole and Benzothiazole: A Concise Review. In *Macromolecular Symposia* 2024, **413(5)**, 2400111.

xix. Dong, X. *Construction of Dynamic DNA Structures for Drug Delivery*. University of California, San Diego, 2021

xx. Fan, Z., Liu, Y., Ye, Y., & Liao, Y. Functional probes for the diagnosis and treatment of infectious diseases. *Aggregate*, 2024, e620.

xxi. Jiang, H., Xi, H., Juhas, M., & Zhang, Y. Biosensors for Point Mutation Detection. *Frontiers in Bioengineering and Biotechnology*, 2021, **9**, 797831.

xxii. Wang, D., Zhang, X., & Zhu, X. Drug-Grafted DNA for Cancer Therapy. *The Journal of Physical Chemistry B*, 2023, **127(24)**, 5379-5388.

xxiii. Rbaa, M., Abousalem, A. S., Galai, M., Lgaz, H., Lakhrissi, B., Warad, I., & Zarrouk, A. New N-heterocyclic compounds based on 8-hydroxyquinoline as

efficient corrosion inhibition for mild steel in hcl solution: experimental and theoretical assessments. *Arabian Journal for Science and Engineering*, 2021, **46**, 257-274.

xxiv. El-Meguid, E. A. A., & Ali, M. M. Synthesis of some novel 4-benzothiazol-2-yl-benzoyl-1 H-pyrazoles, and evaluation as antiangiogenic agents. *Research on Chemical Intermediates*, 2016, **42**, 1521-1536.

xxv. El-Faham, A., & Albericio, F. COMU: A third generation of uronium-type coupling reagents. *Journal of peptide science: an official publication of the European Peptide Society*, 2010, **16(1)**, 6-9.

xxvi. Sur, S. Coupling of single-stranded poly-T DNA with small heterocyclic compounds via peptide linkage, 2024

xxvii. Case, D. A., Aktulga, H. M., Belfon, K., Cerutti, D. S., Cisneros, G. A., Cruzeiro, V. W. D., & Merz Jr, K. M. AmberTools. *Journal of chemical information and modeling*, 2023, **63(20)**, 6183-6191.

xxviii. Gohlke, H., & Case, D. A. Converging free energy estimates: MM-PB (GB) SA studies on the protein–protein complex Ras–Raf. *Journal of computational chemistry*, 2004, **25(2),** 238-250.

xxix. Fujiwara, S. I., & Amisaki, T. Identification of high affinity fatty acid binding sites on human serum albumin by MM-PBSA method. *Biophysical journal*, 2008, **94(1)**, 95-103.

xxx. Tian, C., Kasavajhala, K., Belfon, K. A., Raguette, L., Huang, H., Migues, A. N., & Simmerling, C. (2019). ff19SB: amino-acid-specific protein backbone parameters trained against quantum mechanics energy surfaces in solution. *Journal of chemical theory and computation*, 2019, **16(1),** 528-552.

xxxi. Vassetti, D., Pagliai, M., & Procacci, P. Assessment of GAFF2 and OPLS-AA general force fields in combination with the water models TIP3P, SPCE, and OPC3 for the solvation free energy of druglike organic molecules. *Journal of chemical theory and computation*, 2019, **15(3),** 1983-1995.

xxxii. Cornell, W. D., Cieplak, P., Bayly, C. I., & Kollman, P. A. Application of RESP charges to calculate conformational energies, hydrogen bond energies, and free energies of solvation. *Journal of the American Chemical Society*, 2002, **115(21)**, 9620-9631.

xxxiii. Kumar, P., Nagarajan, A., & Uchil, P. D. Analysis of cell viability by the MTT assay. *Cold spring harbor protocols*, 2018, **6**, pdb-prot095505.

xxxiv. Bahuguna, A., Khan, I., Bajpai, V. K., & Kang, S. C. (2017). MTT assay to evaluate the cytotoxic potential of a drug. *Bangladesh Journal of Pharmacology*, 2017, **12(2),** 115-118.

Received on December 6, 2024.